crystals

MDPI

Article

High-Temperature Electronic Transport Properties of PEDOT:PSS Top-Contact Molecular Junctions with Oligophenylene Dithiols

Dong-Hyoup Seo, Kyungjin Im and Hyunwook Song *

Department of Applied Physics, Kyung Hee University, Yongin 17104, Korea; ehdguq1309@khu.ac.kr (D.-H.S.); limkj0512@khu.ac.kr (K.I.)
* Correspondence: hsong@khu.ac.kr

Abstract: In this study, we investigated the high-temperature electronic transport behavior of spin-coated PEDOT:PSS top-contact molecular ensemble junctions based on self-assembled monolayers (SAMs) of oligophenylene dithiols. We observed irreversible temperature-dependent charge transport at the high-temperature regime over 320 K. The effective contact resistance and normalized resistance decreased with increasing temperature (320 to 400 K), whereas the tunneling attenuation factor was nearly constant irrespective of temperature change. These findings demonstrate that the high-temperature transport properties are not dominated by the integrity of SAMs in molecular junctions, but rather the PEDOT:PSS/SAMs contact. Transition voltage spectroscopy measurements indicated that the contact barrier height of the PEDOT:PSS/SAMs is lowered at elevated temperatures, which gives rise to a decrease in the contact resistance and normalized resistance. The high-temperature charge transport through these junctions is also related to an increase in the grain area of PEDOT cores after thermal treatment. Moreover, it was found that there was no significant change in either the current density or normalized resistance of the annealed junctions after 60 days of storage in ambient conditions.

Keywords: molecular junction; PEDOT:PSS; off-resonant tunneling; transition voltage spectroscopy

Citation: Seo, D.-H.; Im, K.; Song, H. High-Temperature Electronic Transport Properties of PEDOT:PSS Top-Contact Molecular Junctions with Oligophenylene Dithiols. *Crystals* **2022**, *12*, 962. https://doi.org/10.3390/cryst12070962

Academic Editors: Bo Chen, Rutao Wang and Nana Wang

Received: 17 June 2022
Accepted: 8 July 2022
Published: 10 July 2022

1. Introduction

Molecular ensemble junctions have been considered a key element in molecular electronics in which self-assembled monolayers (SAMs) of individual molecules are vertically sandwiched between top and bottom electrodes and the constituent molecules span the two electrodes [1–3]. This junction arrangement typically prefers quantum mechanical tunneling as a charge transport mechanism through SAMs because of their large HOMO–LUMO (the highest occupied and lowest unoccupied molecular orbitals) gap with a very short molecular length [4–6]. Over the past few decades, a variety of pioneering techniques, such as a conducting atomic force microcopy [7], Hg drop [8], eutectic Ga-In [9], nanopore [6], micro-via-hole [5], nanoparticle top-contact [10], metal transfer printing [11], and graphene interlayer [12], have been demonstrated to fabricate and characterize the molecular ensemble junctions based on SAMs. In particular, the highly conducting polymer poly(3,4-ethylenedioxythiophene):ploy(styrenesulfonate) (PEDOT:PSS) top-contact molecular ensemble junction is one of the most successful methods to achieve the high yield of working devices as well as the outstanding stability and reproductivity of large area junctions (up to several hundreds of μm^2 in area) [2,13,14], which are crucial for any technological applications of molecular electronic devices. However, the physisorbed contact properties between the spin-coated PEDOT:PSS top-contact and SAMs have been not thoroughly investigated in the test device platform of molecular junctions. Moreover, most of the charge transport studies on the molecular junction have been performed at low (cryogenic) or room temperature due to its thermal instability [3,13,15].

In this work, we studied the electronic transport properties of PEDOT:PSS top-contact molecular junctions containing oligophenylene dithiols with three different lengths. The PEDOT:PSS top electrodes spin-coated on the SAMs of oligophenylene dithiols effectively prevent electrical shorts from vapor-deposited top metal contacts. The active region of a molecular junction is generated by via-holes photolithographically pattered in photoresist to eliminate parasitical current paths and protect the junction from ambient conditions. The oligophenylene dithiols are one of the simplest prototype molecules with a π-conjugated backbone, which provide a control series to systemically investigate the charge transport through molecular junctions because the off-resonant tunneling mechanism has been coherently demonstrated so far for these molecules [16,17]. Here, our primary focus is on high-temperature charge transport behavior through the annealed PEDOT:PSS molecular junctions. Specifically, we observed that the low-bias junction resistance is temperature-dependent at elevated temperatures above 320 K, which is highly related to total area of the PEDOT grains and the conductivity of spin-coated PEDOT:PSS film. The high-bias nonlinear transport is also examined by transition voltage spectroscopy, indicating that the barrier height at the PEDOT:PSS/SAMs contact is lowered with increasing annealing temperature and therefore the effective contact resistance of these junctions is decreased. Finally, we demonstrate the long-term stability of PEDOT:PSS molecular junctions after thermal treatment.

2. Experimental Details

The device structure of a molecular ensemble junction with the PEDOT:PSS top-contact is schematically shown in Figure 1a. Three different oligophenylene dithiols, abbreviated as OPD-*n*, where *n* denotes the number of a phenyl ring (see Figure 1b), are sandwiched between the PEDOT:PSS (top) and Au (bottom) electrodes. To fabricate the device, a 2 nm thick Ti adhesion layer and a 60 nm thick Au bottom electrode are vapor-deposited on a thermally oxidized Si substrate using an e-beam evaporator. As seen in Figure 1c, a photoresist layer is spin-coated and via-hole arrays of diameter 20–200 μm are created by a typical photolithographic method. For the SAM formation on Au bottom electrodes, the substrate is immersed into an ethanol solution of OPD-*n* molecules at a concentration of 1–2 mM for a minimum of 24 h. Before the next process, it is thoroughly rinsed with clean ethanol and then dried in a vacuum desiccator. The conducting polymer PEDOT:PSS (Clevios^{TM} PH1000) modified with 5% dimethyl sulfoxide (DMSO) is spin-coated on top of the OPD-*n* SAMs, producing a film thickness of 90–100 nm with a conductivity of about 300 S cm^{-1} at room temperature. It has been known that the conductivity of DMSO-modified PEDOT:PSS film is 2–3 orders of magnitude greater than that of pure PEDOT:PSS [13]. Moreover, the pure PEDOT:PSS makes short molecular junctions indistinguishable due to its low conductivity and high contact resistance [14]. In order to secure low contact resistance, a 50 nm Au top-contact pad is vapor-deposited through a shadow mask. Lastly, residual SAMs and PEDOT:PSS film outside the effective region of a molecular junction are eliminated using reactive ion etching, in which the top Au layer acts as an etching mask. All the electrical measurements were performed in a probe station equipped with a built-in temperature controller (MS tech, M5VC model) using a semiconductor parameter analyzer (Keithley 4200A-SCS), where the sample stage cools using a liquid nitrogen. The experimental conditions (e.g., spin-coating and deposition rate and solvent concentrations) are consistently preserved to examine the effect of anneal temperature on charge transport through the molecular junctions. To investigate the long-term stability of annealed molecular junctions, the samples are stored in ambient conditions (usually temperatures of 293–302 K and the relative humidity of 40–50%) without light shielding, humidity control, or any other precautions, and then are remeasured after 60 days in air.

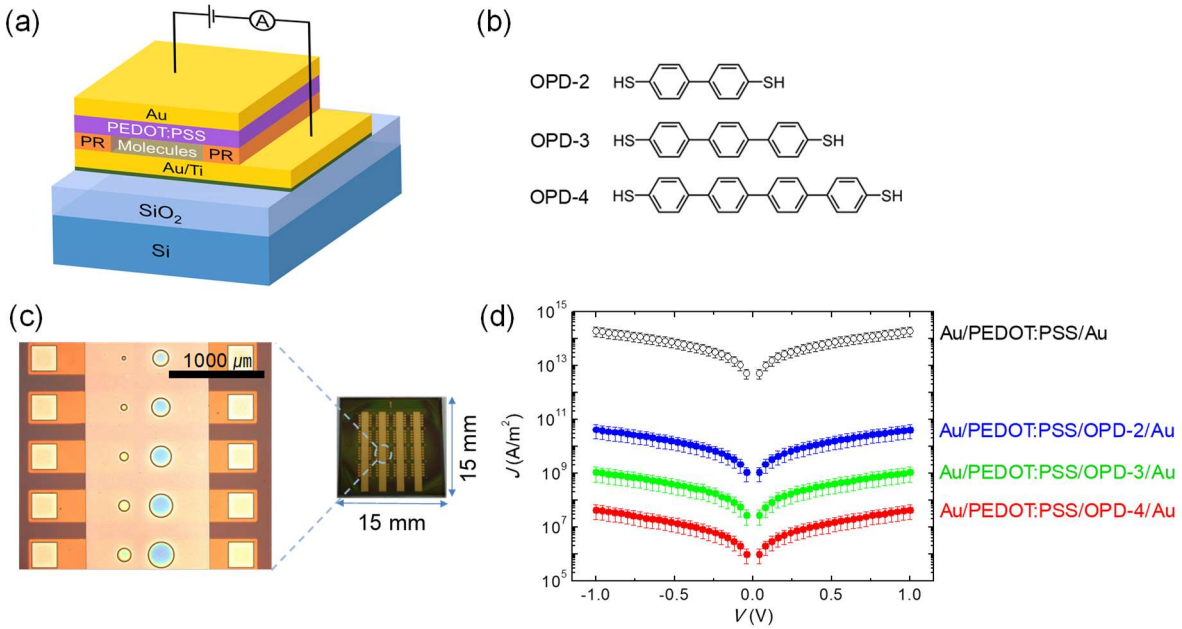

Figure 1. (**a**) Schematic image of PEDOT:PSS top-contact molecular ensemble junctions. (**b**) Chemical structure of oligophenylene dithiols with three different lengths (n = 2, 3 and 4). (**c**) Optical images of fabricated devices, showing via-hole arrays with diameter 20–200 μm. (**d**) Room temperature $J(V)$ curves of OPD-2, OPD-3, OPD-4, and PEDOT:PSS only junctions.

3. Results and Discussion

The oligophenylene dithiols with different lengths constitute an important control series in molecular junctions because it has been unambiguously determined that off-resonant tunneling is the dominant conduction mechanism for these molecules and the length-dependent transport behavior with various electrode systems is extensively reported in studies [1–3], providing a crucial comparative study to validate the demonstration of molecular junctions based on PEDOT:PSS top-contact. Moreover, oligophenylene forms the conjugated backbone of a molecular wire, and the application of such conductive organic molecules as an active component in molecular junctions is highly desirable in the field of molecular electronics. Figure 1d presents the current density (J) of OPD-n (n = 2, 3 and 4) junctions on a logarithmic scale as a function of the bias voltage (V), which was measured at room temperature. The $J(V)$ curves were produced by an average over 20 devices per molecule, and the error bars denote a standard deviation. The ODP-n junction shows a much lower J value than that of a PEDOT:PSS-only device (that is, without ODP-n SAMs). For the case of OPD-2 (the shortest molecule), it was decreased by a factor of ~10^4 in a unit of A/m^2, indicating that a molecular tunnel barrier was formed in the vertically sandwiched junctions. Figure 1d also exhibits that the current density exponentially decreases with increasing n or a molecular length, which can be considered as a typical characteristic of off-resonant tunneling [6,14]. The most remarkable feature observed in the PEDOT:PSS top-contact molecular junctions is that the charge transport exhibits temperature-dependent behavior at a high temperature (typically over room temperature). Figure 2a shows the normalized resistance RA (where R is the resistance and A is the junction area) plotted against the annealing temperature. R is determined by the linear fits of $J(V)$ curves in a low bias region ranging from −0.1 to +0.1 V and the plots are displayed for different molecular lengths of OPD-n in Figure 2a. The RA values of all junctions exponentially decrease with increasing temperature at more than 320 K, whereas those are nearly constant at low temperatures (80–300 K). As clearly shown in Figure 2b, the $J(V)$ characteristics of OPD-n junctions indicate an irreversible change for temperature variation. This result implies that the charge transport properties might be not caused by thermally activated conduction mechanisms or thermal broadening of the Fermi-Dirac distribution at the contacts.

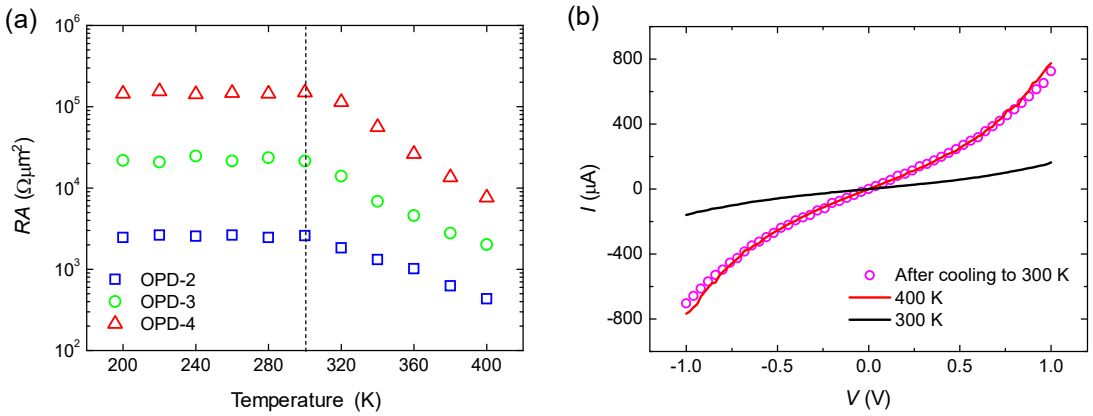

Figure 2. (**a**) Semilog plots of *RA* versus temperature for OPD-*n* junctions at different annealing temperatures (300, 340, and 380 K). A vertically dashed line indicates 300 K. (**b**) Irreversible *I*(*V*) characteristic of OPD-4 junction after thermal annealing at 400 K.

To understand the charge transport properties of PEDOT:PSS top-contact molecular junctions at the high-temperature regime (≥320 K), we performed a variety of transport characterizations, including the measurements of a tunneling attenuation factor β, effective contact resistance R_c, and transition voltage V_{trans} for OPD-*n* molecular series. Figure 3a displays the normalized resistance *RA* against the number of a phenyl ring (n = 2, 3, 4) at different annealing temperatures (300, 340, and 380 K). It was observed that the *RA* values exponentially increase with n. The low-bias resistance R of a molecular tunnel junction is typically expressed as [6,9]:

$$R = R_c \exp(\beta n) \quad (1)$$

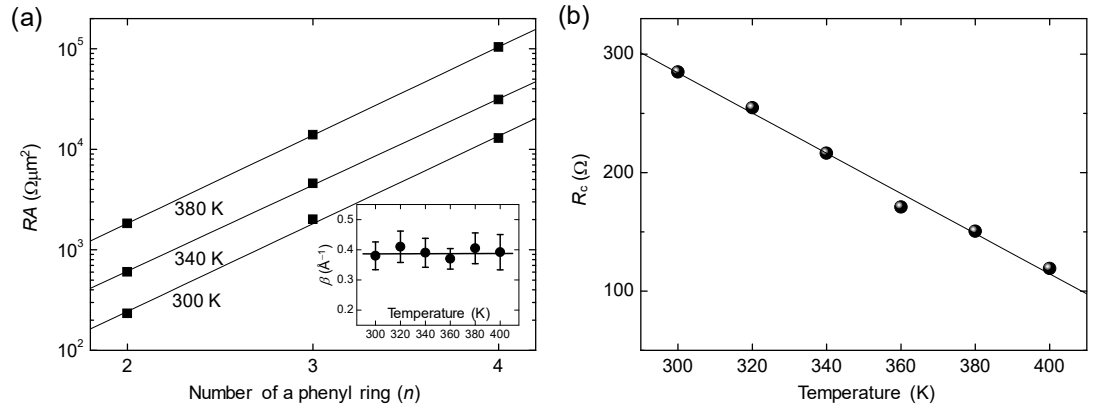

Figure 3. (**a**) Semilog plots of *RA* versus n. Inset shows β values as a function of temperature. Solid lines indicate linear fits. Error bars denote fitting errors. (**b**) Plot of R_c versus temperature. Solid lines indicate a linear fit.

Equation (1) is a general feature of off-resonant tunneling and also convenient because it distinguishes the exponential length dependence of R from the molecule–electrode contact contribution (R_c). β is determined from the slope of linear fits (solid lines) in Figure 3a. It has been well-known that β is a parameter that depends on the molecular backbone structure in the junctions, reflecting the extent to which the electron wave function decays with a molecular length [3,6]. The β value obtained at 300 K is 1.61 per a phenyl ring (=0.38 Å^{-1}), which reasonably agrees with previous studies for OPD-*n* junctions [16,17]. Noticeably, β is nearly constant across a range of annealing temperatures as shown in the inset of Figure 3a. This finding clearly indicates that the efficiency of the tunneling process through the conjugated molecular backbone of OPD-*n* is maintained, thus implying that the integrity of SAMs in the molecular junctions is saved from considerable damage

within the temperature range investigated (up to 400 K). On the contrary, we observed that R_c monotonously decreases with elevating temperature (Figure 3b), which is determined from an extrapolation at n = 0 in Figure 3a using Equation (1). These results indicate that the high-temperature charge transport behavior is not dominated by the integrity of SAMs themselves in the junctions, but rather electrical contacts between PEDOT:PSS top electrodes and OPD-*n* SAMs.

It has been recognized that the morphology of spin-coated PEDOT:PSS films has a core–shell structure consisting of highly-conductive PEDOT cores enclosed by shells with non-conductive PSS chains [18]. The electrical conduction in PEDOT:PSS occurs mainly by charge hopping through PEDOT grains, but not PSS shells. Therefore, the total area of PEDOT segments occupied in the conducting polymer is a crucial factor in determining its conductivity. The grain area of PEDOT conductive regions in the spin-coated PEDOT:PSS film can be examined by its phase image obtained from an atomic force microscopy (AFM) [18]. Figure 4a displays representative AFM topographical and phase images of a PEDOT:PSS film obtained at 300 K and after being annealed at 400 K. A bright (in positive degree) and dark (in negative degree) region in the phase images corresponds to the grains of a PEDOT core and PSS shell, respectively. We obtained all the AFM images after cooling the samples to room temperature and found that the total area of PEDOT grains increases with thermal treatment. For comparison, the PEDOT grain area was calculated to be 0.452 μm^2 at 300 K and 0.538 μm^2 at 400 K in the phase images of 1 μm^2 using a built-in analysis software (see Figure 4a, bottom). Figure 4b shows a direct correlation between the entire grain area of PEDOT cores and four-point-probe conductivity of PEDOT:PSS films with an increase in the annealing temperature from 300 to 400 K. This result demonstrates that high temperatures over 320 K give rise to an increase in the total grain area of conductive PEDOT cores and thus the enhancement of PEDOT:PSS electrode's conductivity. In addition, residual solvent and moisture, acting as a tunnel barrier in the spin-coated PEDOT:PSS top-contact molecular junctions, can be evaporated during an annealing process. These effects generate better electrical contact between the PEDOT:PSS film and OPD-*n* SAMs, leading to a decrease in the normalized resistance (Figure 2a) and effective contact resistance (Figure 3b) of the junctions.

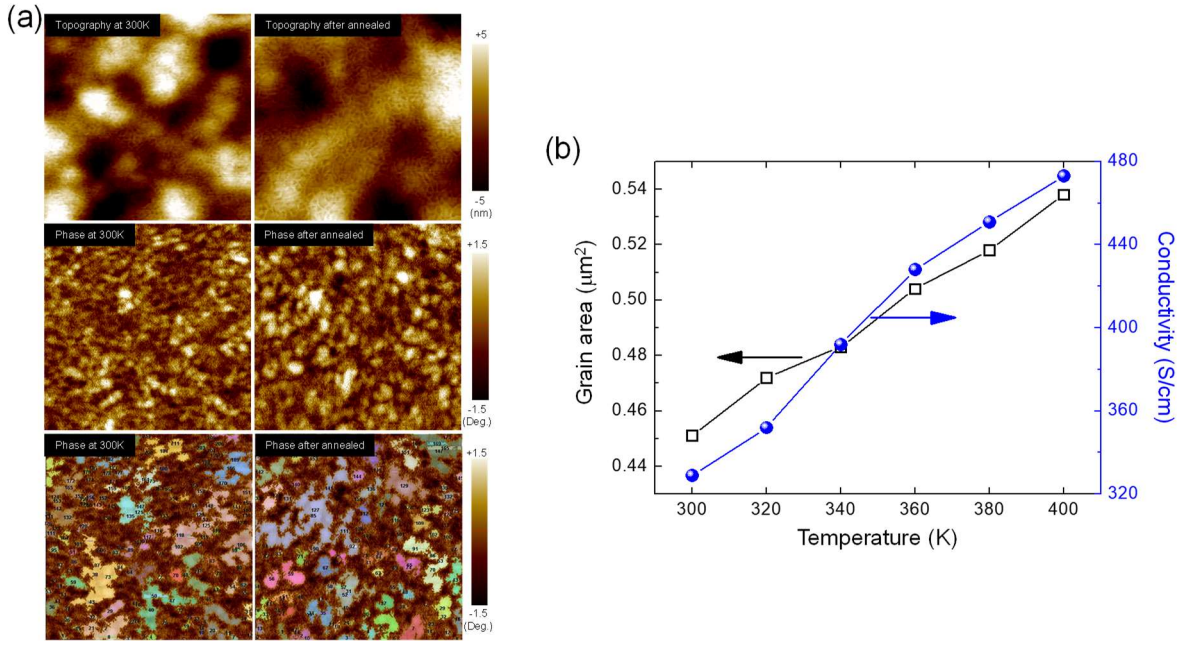

Figure 4. (**a**) AFM topography image (top), phase images (middle), and grain area calculation (bottom) of PEDOT:PSS film in of 1 × 1 μm^2 area obtained at 300 K and after being annealed at 400 K. (**b**) Plots of the total grain area of PEDOT cores and the conductivity of PEDOT:PSS film against temperature.

For a more comprehensive investigation of charge transport behavior through PEDOT:PSS molecular junctions, we also examined the high-bias (nonlinear) regime of the current (I)−voltage characteristics at different temperatures. In a situation of off-resonant tunneling observed in the OPD-*n* junctions, a tunnel barrier can be approximately estimated from the inflection (or transition) voltage $V = V_{trans}$ in a Fowler–Nordheim plot of the same $I(V)$ characteristics [19]. This method is so-called transition voltage spectroscopy (TVS) [20]. Owing to its simplicity and reproducibility, TVS have been widely utilized as a tool to quantify the barrier height for nonlinear transport through molecular tunnel junctions [20–22]. As representatively illustrated in Figure 5a, we examined the shape of nonlinear $I(V)$ curves obtained from OPD-*n* junctions by recasting the curves as Fowler–Nordheim coordinates, that is, $\ln|I^2/V|$ versus $1/V$. These plots produce well-defined minima at V_{trans} (as denoted by arrows in Figure 5a), which is the key quantity of TVS and gives an approximation to the height of tunneling barrier in the junctions. To investigate the influence of thermal treatment on charge transport through the junctions, we plot V_{trans} as a function of temperature in Figure 5b. It was found that V_{trans} consistently decreases for OPD-*n* junctions as temperature increases. A decease in V_{trans} indicates the lowering of a barrier height with high temperature, which can be attributed to a decrease in the effective contact resistance at the interface between PEDOT:PSS and OPD-*n* due to an increase in the grain area of PEDOT cores (as described in Figure 4) and the removal of residual solvent and water in the spin-coated polymer films.

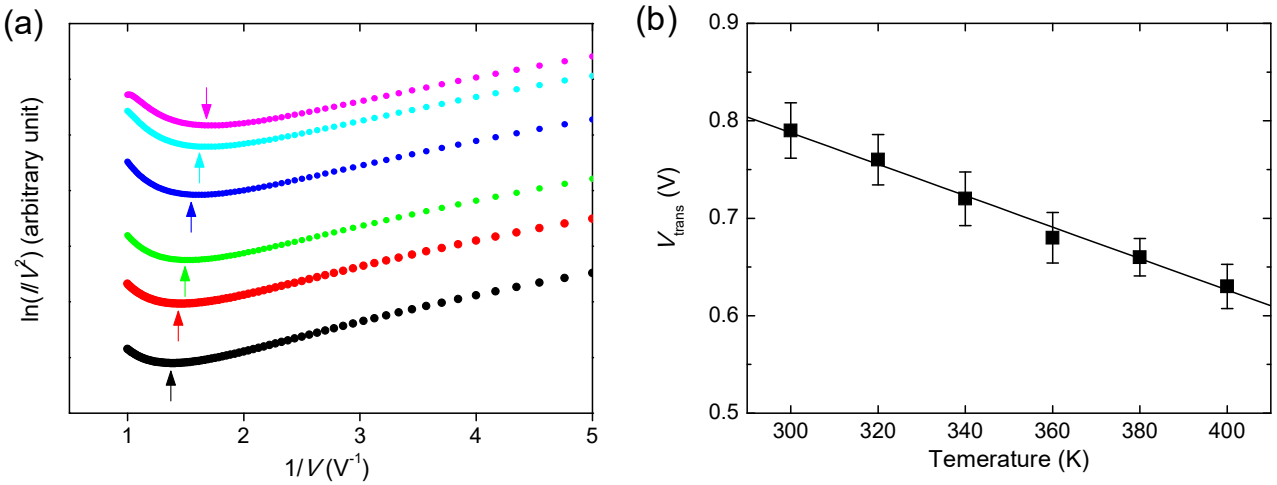

Figure 5. (**a**) Fowler–Nordheim plots of OPD-*n* junctions. Arrows indicate V_{trans}. (**b**) Plot of V_{trans} versus temperature. Solid line indicates a linear fit and error bars denote a standard deviation.

Furthermore, to examine the long-term stability of PEDOT:PSS molecular junctions with high temperature, the samples were annealed at 400 K and then stored in ambient conditions for subsequent electrical measurements. We remeasured the junctions after 60 days. As shown in Figure 6a, there is no significant change in the $J(V)$ curves. A slight decrease in the current density is probably due to an increase in the hopping distance of PEDOT:PSS films or an additional contact barrier resulting from water molecules in air [18]. Figure 6b presents the RA values of eight distinct junctions after 2 months of storage in ambient conditions, where the only small increase in RA values was observed for all measured devices.

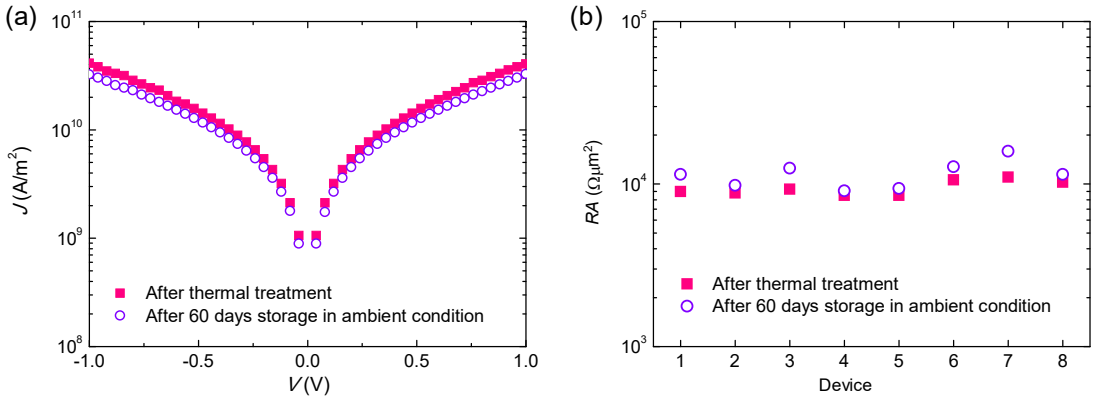

Figure 6. (**a**) The $J(V)$ characteristics of OPD-2 junctions measured after being annealed at 400 K and 60 days of storage in ambient conditions. (**b**) RA values for 8 OPD-2 junctions measured after being annealed at 400 K and 60 days of storage in ambient conditions.

4. Conclusions

We investigated the charge transport properties of spin-coated PEDOT:PSS top-contact molecular ensemble junctions with OPD-*n* SAMs. The current density exponentially decreased with molecular length, indicating a general feature of off-resonant tunneling. The charge transport exhibited irreversible temperature-dependent behavior at the high-temperature regime. The normalized resistance rapidly decreased with increasing temperature above 320 K. β showed a constant value of 0.38 Å^{-1}, whereas R_c linearly decreased as temperature increases from 320 to 400 K. These results indicate that the high-temperature transport behavior was dominated by the PEDOT:PSS/SAMs contact, but not the integrity of SAMs in the junctions. A decease in V_{trans} can be attributed to the contact barrier lowering at the PEDOT:PSS/SAMs interface, which is most probably due to an increase in the grain area of PEDOT cores and the removal of residual solvent and water in the spin-coated polymer films after thermal annealing. In addition, no significant change was found in the current density and normalized resistance of the annealed molecular junctions after 60 days of storage in ambient conditions. Recent studies also indicate that PEDOT:PSS electrodes can provide various approaches to create molecular junctions [23–25].

Author Contributions: Conceptualization, H.S.; Investigation, D.-H.S. and K.I.; Methodology, D.-H.S. and K.I.; Supervision, H.S.; Writing–original draft, H.S.; Writing–review & editing, D.-H.S., K.I. and H.S. All authors have read and agreed to the published version of the manuscript.

Funding: This work was supported by the National Research Foundation of Korea (grant No. 2020R1F1A1076107).

Institutional Review Board Statement: Not applicable.

Informed Consent Statement: Not applicable.

Data Availability Statement: Data is contained within the article.

Conflicts of Interest: The authors declare no conflict of interest.

References

1. Liu, Y.; Qiu, X.; Soni, S.; Chiechi, R.C. Charge Transport through Molecular Ensembles: Recent Progress in Molecular Electronics. *Chem. Phys. Rev.* **2021**, *2*, 021303. [CrossRef]
2. Vilan, A.; Aswal, D.; Cahen, D. Large-Area, Ensemble Molecular Electronics: Motivation and Challenges. *Chem. Rev.* **2017**, *117*, 4248–4286. [CrossRef]
3. Xiang, D.; Wang, X.; Jia, C.; Lee, T.; Guo, X. Molecular-Scale Electronics: From Concept to Function. *Chem. Rev.* **2016**, *116*, 4318–4440. [CrossRef]
4. Jeong, H.; Kim, D.; Xiang, D.; Lee, T. High-Yield Functional Molecular Electronic Devices. *ACS Nano* **2017**, *11*, 6511–6548. [CrossRef]

5. Song, H.; Lee, T.; Choi, N.-J.; Lee, H. A statistical method for determining intrinsic electronic transport properties of self-assembled alkanethiol monolayer devices. *Appl. Phys. Lett.* **2007**, *91*, 253116. [CrossRef]
6. Wang, W.; Lee, T.; Reed, M.A. Mechanism of electron conduction in self-assembled alkanethiol monolayer devices. *Phys. Rev. B* **2003**, *68*, 035416. [CrossRef]
7. Wold, D.J.; Frisbie, C.D. Formation of Metal-Molecule-Metal Tunnel Junctions: Microcontacts to Alkanethiol Monolayers with a Conducting AFM Tip. *J. Am. Chem. Soc.* **2000**, *122*, 2970–2971. [CrossRef]
8. Holmlin, R.E.; Haag, R.; Chabinyc, M.L.; Ismagilov, R.F.; Cohen, A.E.; Terfort, A.; Rampi, M.A.; Whitesides, G.M. Electron Transport through Thin Organic Films in Metal−Insulator−Metal Junctions Based on Self-Assembled Monolayers. *J. Am. Chem. Soc.* **2001**, *123*, 5075–5085. [CrossRef]
9. Yuan, L.; Jiang, L.; Zhang, B.; Nijhuis, C.A. Dependency of the Tunneling Decay Coefficient in Molecular Tunneling Junctions on the Topography of the Bottom Electrodes. *Angew. Chem. Int. Ed.* **2014**, *53*, 3377–3381. [CrossRef]
10. Puebla-Hellmann, G.; Venkatesan, K.; Mayor, M.; Lörtscher, E. Metallic nanoparticle contacts for high-yield, ambient-stable molecular-monolayer devices. *Nature* **2018**, *559*, 232–235. [CrossRef]
11. Jeong, H.; Kim, D.; Kim, P.; Cho, M.R.; Hwang, W.-T.; Jang, Y.; Cho, K.; Min, M.; Xiang, D.; Park, Y.D.; et al. A new approach for high-yield metal–molecule–metal junctions by direct metal transfer method. *Nanotechnology* **2015**, *26*, 025601. [CrossRef]
12. Park, S.; Kim, H.R.; Kim, J.; Hong, B.-H.; Yoon, H.J. Enhanced Thermopower of Saturated Molecules by Noncovalent Anchor-Induced Electron Doping of Single-Layer Graphene Electrode. *Adv. Mater.* **2021**, *33*, 2103177. [CrossRef]
13. Akkerman, H.B.; Blom, P.W.M.; de Leeuw, D.M.; de Boer, B. Towards molecular electronics with large-area molecular junctions. *Nature* **2006**, *441*, 69–72. [CrossRef]
14. Akkerman, H.B.; Naber, R.C.G.; Jongbloed, B.; van Hal, P.A.; Blom, P.W.M.; de Leeuw, D.M.; de Boer, B. Electron tunneling through alkanedithiol self-assembled monolayers in large-area molecular junctions. *Proc. Natl. Acad. Sci. USA* **2007**, *104*, 11161–11166. [CrossRef]
15. Kühnel, M.; Overgaard, M.H.; Hels, M.C.; Cui, A.; Vosch, T.; Nygård, J.; Li, T.; Laursen, B.W.; Nørgaard, K. High-Quality Reduced Graphene Oxide Electrodes for Sub-Kelvin Studies of Molecular Monolayer Junctions. *J. Phys. Chem. C* **2018**, *122*, 25102–25109. [CrossRef]
16. Nguyen, Q.V.; Xie, Z.; Frisbie, C.D. Quantifying Molecular Structure-Tunneling Conductance Relationships: Oligophenylene Dimethanethiol vs Oligophenylene Dithiol Molecular Junctions. *J. Phys. Chem. C* **2021**, *125*, 4292–4298. [CrossRef]
17. Xie, Z.; Bâldea, I.; Frisbie, C.D. Determination of Energy-Level Alignment in Molecular Tunnel Junctions by Transport and Spectroscopy: Self-Consistency for the Case of Oligophenylene Thiols and Dithiols on Ag, Au, and Pt Electrodes. *J. Am. Chem. Soc.* **2019**, *141*, 3670–3681. [CrossRef]
18. Nardes, A.M.; Janssen, R.A.J.; Kemerink, M. A Morphological Model for the Solvent-Enhanced Conductivity of PEDOT:PSS Thin Films. *Adv. Funct. Mater.* **2008**, *18*, 865–871. [CrossRef]
19. Beebe, J.M.; Kim, B.; Gadzuk, J.W.; Frisbie, C.D.; Kushmerick, J.G. Transition from Direct Tunneling to Field Emission in Metal-Molecule-Metal Junctions. *Phys. Rev. Lett.* **2006**, *97*, 026801. [CrossRef]
20. Beebe, J.M.; Kim, B.; Frisbie, C.D.; Kushmerick, J.G. Measuring Relative Barrier Heights in Molecular Electronic Junctions with Transition Voltage Spectroscopy. *ACS Nano* **2008**, *2*, 827–832. [CrossRef]
21. Chen, J.; Markussen, T.; Thygesen, K.S. Quantifying Transition Voltage Spectroscopy of Molecular Junctions: Ab Initio Calculations. *Phys. Rev. B* **2010**, *82*, 121412. [CrossRef]
22. Nose, D.; Dote, K.; Sato, T.; Yamamoto, M.; Ishii, H.; Noguchi, Y. Effects of Interface Electronic Structures on Transition Voltage Spectroscopy of Alkanethiol Molecular Junctions. *J. Phys. Chem. C* **2015**, *119*, 12765–12771. [CrossRef]
23. Bruce, J.P.; Oliver, D.R.; Lewis, N.S.; Freund, M.S. Electrical Characteristics of the Junction between PEDOT:PSS and Thiophene-Functionalized Silicon Microwires. *ACS Appl. Mater. Interfaces* **2015**, *7*, 27160–27166. [CrossRef]
24. Yildirim, E.; Zhu, Q.; Wu, G.; Tan, T.L.; Xu, J.; Yang, S.-W. Self-Organization of PEDOT:PSS Induced by Green and Water-Soluble Organic Molecules. *J. Phys. Chem. C* **2019**, *123*, 9745–9755. [CrossRef]
25. Zhu, Q.; Yildirim, E.; Wang, X.; Soo, X.Y.D.; Zheng, Y.; Tan, T.L.; Wu, G.; Yang, S.-W.; Xu, J. Improved Alignment of PEDOT:PSS Induced by in-situ Crystallization of "Green" Dimethylsulfone Molecules to Enhance the Polymer Thermoelectric Performance. *Front. Chem.* **2019**, *7*, 783. [CrossRef]